Far-Infrared Band Strengths in the Water Dimer: Experiments and Calculations

Justinas Ceponkus,* Per Uvdal, and Bengt Nelander

Chemical Physics, P.O. Box 124 and MAX- lab, P.O. Box 118, Lund University, SE-22100 Lund, Sweden

Received: November 26, 2007; In Final Form: January 17, 2008

Most fundamentals modes of the water dimer have been experimentally determined, and the frequencies have been measured in either neon or parahydrogen matrices. The band strengths of all intramolecular and most intermolecular fundamentals of the water dimer have been measured. The results are further corroborated by comparison with the corresponding data for the fully deuterated water dimer. DFT calculations of the mode frequencies and band strength are in qualitative agreement with the experimental observations.

Introduction

If we want to describe liquid and solid water from first principles, it will be necessary to have an almost completely correct description of the water dimer as a start. Also, if one aims toward a molecular understanding of solid and liquid water, the intermolecular dimer modes will be of particular importance. In the present work., we present almost complete vibrational spectra of the water dimer for these important modes. The experimental data are compared with first-principle calculations performed at the anharmonic level.

The first experimental observation of the water dimer was reported by Pimentel and co-workers,[1] who used infrared spectroscopy to test the trapping ability of nitrogen matrices. Later infrared spectroscopic studies of matrix-isolated water at higher resolution made it clear that the water dimer is linear with one water as proton acceptor and the other as proton donor.[2−4] Dyke and co-workers used microwave spectroscopy on molecular beams to establish the linear structure of the dimer and to give an estimate of its O−O distance.[5] Ab initio calculations supported the linear structure[6] and gave estimates of the barriers between the eight equivalent minima on the dimer potential energy surface.[7] The frequencies of most of the intramolecular fundamentals of the gaseous H_2O−HOH dimer and some D_2O−DOD dimer bands have been measured in molecular beams.[8−10] A combination of tera-Herz spectroscopy and microwave spectroscopy on water in molecular beams by Saykally and co-workers[11−13] and theoretical calculations by van der Avoird and his group[14] give a detailed picture of the isomerization of the dimer and of its vibration spectrum below 150 cm^{-1}. The first study of the far-infrared spectrum of the matrix-isolated water dimer was published by Bentwood et al.,[15] who gave data for H_2O−HOH in nitrogen and argon matrices. Recently, two studies of the far-infrared spectrum of the water dimer in neon matrices have been published[16,17]

Almost all previous experimental work on the water dimer has been concerned with the positions of its vibration bands, whereas essentially no work has been done to determine or estimate band intensities. These intensities are important experimental input for the further development of the theoretical modeling of hydrogen-bonding systems. In addition, the water dimer appears to be an important species in the atmosphere,[18−20] where it may influence the energy balance of the earth. Its concentration is low, but the long paths of direct sunlight and of heat radiation from the earth through the atmosphere and the possibility that the dimer absorption may fill holes in the water monomer spectrum make it necessary to establish its importance. Zilles and Person[21] used published matrix isolation spectra to estimate the relative intensities in the intramolecular fundamentals. These estimates and similar estimates in ref 11 represent the only published intensity data on the water dimer. We have estimated the band strengths of the water dimer in parahydrogen and neon matrices. Both parahydrogen and neon can be used to obtain millimeter-thick matrices of high optical quality with minimal baseline problems.

The matrix thickness of a solid parahydrogen matrix can be obtained from its infrared spectrum.[22] It is then possible to estimate the water monomer concentrations in the matrix using gas-phase intensity data. The fact that the spectrum of the acceptor part of the dimer is only slightly perturbed by the dimer formation makes it possible to give reasonably accurate estimates of the dimer concentration from the intensities of the acceptor fundamentals combined with gas-phase monomer band strengths. By using an identical deposition geometry for parahydrogen and neon experiments, neon matrices with known matrix thickness could be prepared, assuming that the matrix growth rates are essentially the same for the different matrices. This has made it possible to give estimates of monomer and dimer concentrations also in neon where no matrix absorption is present.

Experimental Section

The cryostat used in this work is a small immersion helium cryostat, (IHC-3) from the Estonian Academy of Sciences (Dr. Ants Lômus), modified for matrix work. The cryostat can operate from approximately 2.5 to 300 K. The matrix is deposited on a gold-plated OFHC copper mirror. In order to allow the study of thick matrices, a three mm deep, 10 mm diameter cavity with a flat bottom is drilled in the center of the mirror. The mirror temperature is measured with a Lake Shore silicon diode. The temperature of the matrix mirror was stable within less than 0.1 K using feed-back electronics. The outer shroud has a valve through which the depositions are performed. In order to reduce the heat load on the cryostat, the matrix gas

* Permanent address: Department of General Physics and Spectroscopy, Universiteto str.3 LT-01513, Vilnius, Lithuania.

10.1021/jp711178w CCC: $40.75
Published on Web 03/19/2008

is precooled with liquid nitrogen before entering the cryostat. The water is deposited from a separate volume, kept at 273 K with ice-water, through a needle valve and a separate stainless steel tube parallel to the inlet tube for matrix gas. Before deposition, the valve on the shroud is opened and the deposition tubes are slid into the cryostat to a well-defined position ~10 mm from the cavity in the mirror. After deposition, the tubes are withdrawn and the valve is closed. The cryostat is used here to study almost three mm thick parahydrogen matrices with no particular difficulties. This setup also makes it possible to record spectra over the entire infrared region for one deposition using interchangeable CsI and TPX windows.

The matrices were deposited at 3.6 K. The deposition speed was kept constant by keeping the temperature of the matrix mirror constant by adjusting the matrix gas flow. In all but one experiment, approximately 100 mbar of neon or parahydrogen from a 10 L volume was deposited in about 1 h. In one parahydrogen experiment, we deposited twice this amount of gas in 2 h. The same deposition geometry was used for neon and parahydrogen experiments.

Water was doubly distilled and degassed and D_2O (Norsk hydro 99.5%D) was degassed. In a few experiments, $H_2{}^{18}O$ was used. Neon (L'Air Liquide 99.5%) was used as received. Apart from traces of carbon dioxide and water, no infrared absorption was observed in an almost 1 mm thick pure neon matrix. Hydrogen (AGA) was used as received. Infrared spectra of almost two mm thick matrices showed only the presence of traces of carbon dioxide and water.

The para/ortho-hydrogen conversion was performed in a stainless steel tube. The bottom of the tube was filled with a paramagnetic catalyst (iron(III) oxide, catalyst grade, Aldrich Chemical Co.). The tube inlet was connected to a 10 L volume filled with the desired amount of normal hydrogen. The inlet and outlet of the tube are connected in such a way that the gas coming from the inlet has to pass the catalyst to reach the outlet. The tube was immersed in a liquid helium dewar, and the gas from the inlet volume was condensed on the catalyst. Hydrogen was kept condensed on the catalyst for close to 20 min. Then the catalyst was warmed to approximately 15 K by taking the tube just above the surface of the liquid He. The outlet from the conversion tube was collected in a separate volume.

Spectra were recorded with a Bruker HR120 FTIR spectrometer at 0.1 cm^{-1} resolution in the mid-infrared spectrum and at 1 cm^{-1} resolution below 650 cm^{-1}. A Ge/KBr beamsplitter and an MCT detector operating above 650 cm^{-1} (Judson) was used in the mid-infrared region and a specially coated mylar beamsplitter and a helium-cooled Si bolometer (Infrared Laboratories) with cutoff filters at 700 cm^{-1} (used for the CsI region) and at 350 cm^{-1} (used for the TPX region) in the far-infrared region. In a few experiments, a 75 micron mylar beam splitter was used to obtain spectra down to 10 cm^{-1}, with the normally used, coated beamsplitter, spectra down to 20 cm^{-1} were obtained. Spectra of parahydrogen matrices were recorded at 2.8 K. Neon matrix spectra were recorded at temperatures from 2.8 up to 10 K. Intensity measurements were carried out on the 2.8 K spectra.

In the parahydrogen experiments, we used absorption bands of parahydrogen to estimate the matrix thickness.[22] The water monomer concentration was then obtained from the integrated intensities of the water fundamentals using gas-phase band strengths.[23] In most experiments, only the symmetric stretch had a sufficiently low intensity to allow measurement. In those cases where simultaneous significant measurements of all three fundamentals were possible, the concentration estimates differed by at most 30%. Most of this uncertainty is due to the large intensity difference between the symmetric stretch and the two other water fundamentals, which makes it difficult to measure all three on the same sample. The parahydrogen matrix thickness varied between 1.6 and 1.8 mm except in one experiment where we deposited a larger quantity of parahydrogen to give a 2.6 mm thick matrix. Using data for solid neon and for solid parahydrogen, we estimated the matrix thickness in the neon experiments from the amount of neon deposited. The neon matrix thickness was 0.95 mm in the present experiments.

It is well-known that the fundamentals of the proton acceptor in the water dimer shift by small amounts from their monomer values. In order to measure the dimer concentration, we have to make an assumption about dimer band strengths. The symmetric stretch is rather weak and inconvenient for intensity measurements. The asymmetric stretch is difficult to observe since it occurs in a region of strong monomer absorption. It also appears to be temperature-dependent. Fortunately, the acceptor band gives a relatively sharp band, free of disturbing interferences. The full width at half-maximum is 0.46 cm^{-1} in neon and wider in parahydrogen. We used the integrated intensity of this band together with the monomer band strength to estimate the dimer concentration. Our calculations support the assumption that the change of the band strength is relatively small between monomer and proton acceptor.

Nomenclature

The intramolecular water dimer fundamentals are given as $\nu_{n\mathrm{A}}$ or $\nu_n(H_2O{-}HOH)$ for the acceptor and as $\nu_{n\mathrm{D}}$ or $\nu_n(HOH{-}OH_2)$ for the donor part of the dimer. The intermolecular fundamental where the donor part of the dimer librates around its free OH bond is denoted as out-of-plane bend. The in-plane bend is the intermolecular fundamental where the donor part of the dimer librates in the water dimer plane around an axis orthogonal to the water plane at its center of mass.[24] The stretching fundamental is the intermolecular vibration with the largest O−O amplitude.

Calculations

The calculations for the water monomer and the water dimer were preformed using the Gaussian03 package[25] and the density functional method B3LYP. The "full" basis set 6-311++G-(3df,3pd) was used along with the tight convergence criteria and an ultrafine grid for the optimization. The molecular frequencies for both water and fully deuterated water were calculated at both the harmonic and anharmonic level, whereas the intensities could only be calculated at the harmonic level. Fermi and Darling−Dennison resonance interactions were not included in the present calculations (the TolFreq keyword was set to 0.1 cm^{-1}). The calculations for water monomers and water dimers and the corresponding fully deuterated species are compared with experimental results in Tables1−3.

The optimized geometry, shown in Figure 1, is in agreement with what has been obtained previously at this level of calculations. The O−O distance is 2.915 Å and the acceptor O−H bonds are 0.962 Å. The two different donor bonds are 0.969 and 0.960 Å, respectively, the latter being the free hydrogen. The same H−O−H bond angle, 105.4°, was obtained for both the acceptor and the donor.

A comprehensive study of the water dimer using a variety of different density functional theories has been performed by Goddard and co-workers.[26] Most functionals compare quite well with the "complete" coupled cluster calculation using 275 basis functions for the water dimer by Klopper et al.[27] In the latter

TABLE 1: Calculated and Measured Intensities of Monomeric Water[a]

		gas phase		DFT[d]		matrix Ne[e]	matrix p-H$_2$[e]
	mode	ν[b]	S[c]	ν	S	ν	ν
				H_2O			
1	ν_3	3755.79	7.99	3727	10.0	3759.5	3742.8
2	ν_1	3656.65	0.362	3641	0.8	3665.4	3646.0
3	ν_2	1594.59	10.6	1573	12.0	1595.4	1592.9
				D_2O			
1	ν_3	2788.05	4.86	2767	6.0	2790.0	2777.8
2	ν_1	2671.46	0.340	2659	0.6	2676.8	2662.8
3	ν_2	1178.33	5.64	1162	6.4	1178.9	1176.5

[a] Frequencies in cm^{-1}, and band strengths, S, in 10^{18} cm/molecule. [b] Ref 31. [c] Ref 23. [d] This work, anharmonic frequencies. [e] This work.

TABLE 2: Calculated and Measured Band Frequencies and Band Strengths of H_2O-HOH[a]

		Ne		p-H$_2$		DFT[c]	
	mode[b]	ν	S	ν	S	ν	S
1	ν_{3A}	3763.3	8.4	3745.7	5.0	3720	13.6
2	ν_{3D}	3733.6	13	3716.9	19	3707	13.4
3	ν_{1A}	3660.6	1.6	3642.1	1.0	3638	1.7
4	ν_{1D}	3590.5	30	3579.3	38	3555	55
5	ν_{2D}	1616.4	1.5	1613.2	8	1593	6.5
6	ν_{2A}	1599.2	(10.6)[d]	1597.2	(10.6)[d]	1585	15
7	out-of-plane-bend	522.4	18	485		515	17
8	in-plane-bend	309.1	11	299.1	4.5	307	9
9	O−O stretch	173	2.6			124[e]	36
10	"150"	151	3	145.9		118[e]	12.3
11	"122"	122.2	20	121.2	10	117	1.5
12	"76"			75.7	3.6	78	27

[a] Band positions, ν, cm^{-1}; intensities, S, 10^{-18} cm/molecule. [b] ν_{1A}: $\nu_1(H_2O-HOH)$, ν_{1D}: ν (HOH−OH$_2$), ν_{2A}: $\nu(H_2O-HOH)$, ν_{2D}: ν(HOH−OH$_2$), ν_{3A}: $\nu_3(H_2O-HOH)$, ν_{3D}: ν_3(HOH−OH$_2$); out-of-plane-bend, in-plane-bend and stretch, see nomenclature above. [c] This work, anharmonic frequencies. [d] Assumed to be equal to the intensity of the corresponding monomer band (see text). [e] O−O.

TABLE 3: Calculated and Measured Band Frequencies and Band Strengths of D_2O-DOD[a]

		Ne		p-H$_2$		DFT[c]	
	mode[b]	ν	S	ν	S	ν	S
1	ν_{3A}	2790.4	1.8	2774	1.8	2773	7.9
2	ν_{3D}	2762.6	14	2751.6	14	2742	11.6
3	ν_{1A}	2672.7	2.1	2660.3	0.89	2656	1.3
4	ν_{1D}	2625.9	16	2617.5	18	2601	26.0
5	ν_{2D}	1192.2	2.3	1190	2.9	1176	3.7
6	ν_{2A}	1181.6	(5.64)[d]	1180.2	(5.64)[d]	1170	7.8
7	out-of-plane-bend	393.2	9.3			396	9.4
8	in-plane-bend	233.5	3.5			246	5.2
9	O−O stretch	166	6.0			145	7.2
10						105	19
11						100	0.4
12						83	15

[a] Band positions, ν, cm^{-1}; intensities, S, 10^{-18} cm/ molecule. [b] ν_{1A}: $\nu_1(D_2O-DOD)$, ν_{1D}: ν (DOD−OD$_2$), ν_{2A}: $\nu(D_2O-DOD)$, ν_{2D}: ν(DOD−OD$_2$), ν_{3A}: $\nu_3(D_2O-DOD)$, ν_{3D}: ν_3(DOD−OD$_2$); out-of-plane-bend, in-plane-bend and stretch, see nomenclature above. [c] This work, anharmonic frequencies. [d] Assumed to be equal to the intensity of the corresponding monomer band (see text).

calculation, a O−O distance of 2.912 Å was found. The acceptor O−H bonds were 0.958 Å, and the two different donor bonds were 0.964 and 0.957 Å, respectively, the latter being the free hydrogen. The orientation with respect to the O−O axis, as defined in Figure 1, of the acceptor was determined to be 55.6° and for the donor to be 5.5°. That is, all values are in good agreement with the present calculation.

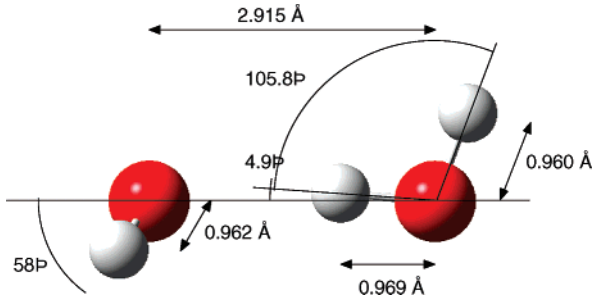

Figure 1. Optimized water dimer geometry.

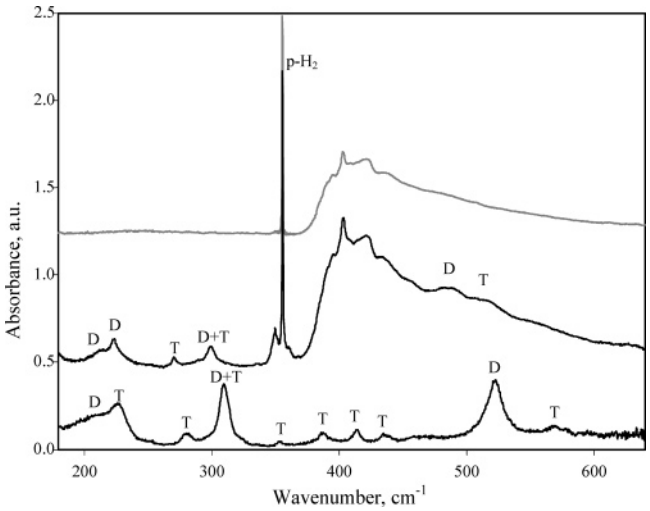

Figure 2. The far-infrared spectrum between 200 and 640 cm^{-1} of water-doped neon, compared to parahydrogen and water-doped parahydrogen. $T = 2.8$ K. Lower curve: neon matrix [Ne]/[H_2O] = 2030. Middle curve: parahydrogen matrix [p-H_2]/ [H_2O] = 388. Upper (gray) curve: parahydrogen without added water. D: dimer, T: trimer, pH_2: parahydrogen zero phonon line.

For comparison, Goldman et al.[28] estimated an O−O distance of 2.952 Å from a parametrized potential surface fitted to an extensive experimental data set. The hydrogen bond deviates 2.3° from linearity according to the same data. In this approach, the individual water molecules were frozen at the monomer equilibrium geometry.

Results and Discussion

The experimental spectra in the far-infrared region of the water dimer, labeled D (and trimers labeled T)), in neon and parahydrogen matrices are presented in Figures 2 and 3. In Figure 2, the data obtained using the CsI window are shown, and the corresponding data using the TPX window are shown in Figure 3. For reference, a spectrum of a neat parahydrogen matrix is included in Figure 2. Both neon and parahydrogen matrix spectra show the presence of the water trimer in addition to the dimer. The assignment of bands to the dimer or trimer was based on their concentration dependencies. In addition, the trimer bands show significant irreversible increases in intensity when the neon matrix is heated to 9 K. Tables 2 and 3 give line positions and band strengths both for the far-infrared and for the intramolecular stretch and bending bands of the mid-infrared region.

There is a close correspondence between the water dimer spectra observed for parahydrogen and neon matrices in the mid-infrared, Tables 2 and 3. The vibrational frequencies are consistently slightly higher in the neon matrix. In the upper part ($\geq$400 cm^{-1}) of the far-infrared spectrum, there are however some differences. We attribute these differences to properties

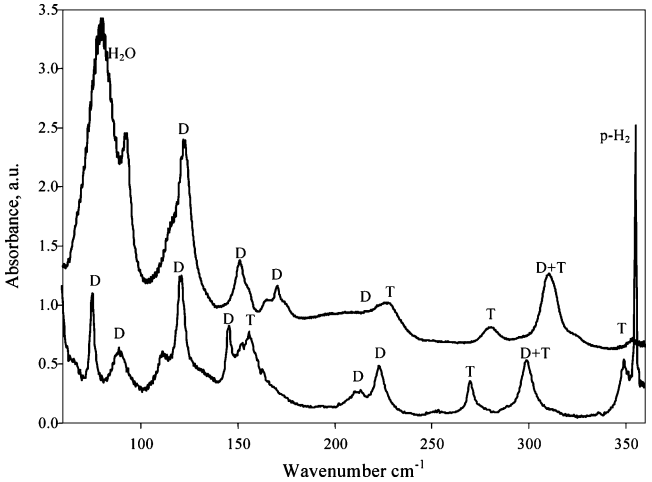

Figure 3. The far-infrared absorption of water-doped neon and parahydrogen matrices below 360 cm^{-1}. $T = 2.8$ K. Upper curve: neon matrix [Ne]/[H_2O] = 1740, lower curve: parahydrogen matrix [p-H_2]/[H_2O] = 340. H_2O: monomer H_2O, D: dimer, T: trimer, pH_2: parahydrogen zero phonon line.

of the two matrices. The hydrogen molecules in solid parahydrogen are in the rotational ground state. Interactions in the solid makes the $J = 0$ to $J = 2$ transition allowed in the far-infrared. The observed band has a sharp zero phonon line at 355.6 cm^{-1} and a broad phonon wing at higher wavenumbers, Figure 2. Unfortunately, the phonon wing obscures this interesting part of the water dimer spectrum. In the presence of water, one observes a broad peak around 488 cm^{-1}, on the high-frequency part of the phonon wing. This peak correlates with the water dimer bands and is close to the out-of-plane bending mode in the calculations at 515 cm^{-1}, Table 2. In neon matrices this band is observed at 522.1 cm^{-1}.

The intermolecular fundamental in-plane bending mode is observed at 309.5 cm^{-1} in neon and at 299.3 cm^{-1} in parahydrogen, Figure 2. The frequency of this mode is calculated to be 307 cm^{-1}, again in agreement with the experimental data, Table 2. This band has some contributions from the trimer as well. The band is present at concentrations where there is virtually no trimer present, but it increases in intensity with water concentration more rapidly than other dimer bands. In addition, its position shifts from 309.5 to 310.8 cm^{-1} when the water concentration increases.

Below the rotation band of the parahydrogen matrix, there is again a close correspondence between the dimer spectra in parahydrogen and neon matrices (see Figure 3), Water monomer has a strong band at 79.5 cm^{-1} in solid neon.[29] This band is absent in parahydrogen, and here we observe a dimer band at 75.9 cm^{-1} with a satellite at 81 cm^{-1}.

The following provides a summary of known sources of errors for the intramolecular H_2O-HOH modes. Similar considerations apply also to the D_2O-DOD measurements.

The integrals over the mode 2, $\nu_3(HOH-OH_2)$, band in neon include a contribution from the $0_{00} \leftarrow 1_{01}$ component of the monomer ν_3 band. It is easy to correct for this overlap since we can measure the integrated intensity of the $2_{02} \leftarrow 1_{01}$ component. The intensity ratio between this component and the $0_{00} \leftarrow 1_{01}$ component is constant and has been obtained from experiments at low concentrations, where no dimer is present. We have not been able to measure the intensity ratio between the two monomer lines in parahydrogen matrices since the $0_{00} \leftarrow 1_{01}$ component is difficult to observe at low water concentrations. We therefore assume that the neon ratio can be used also

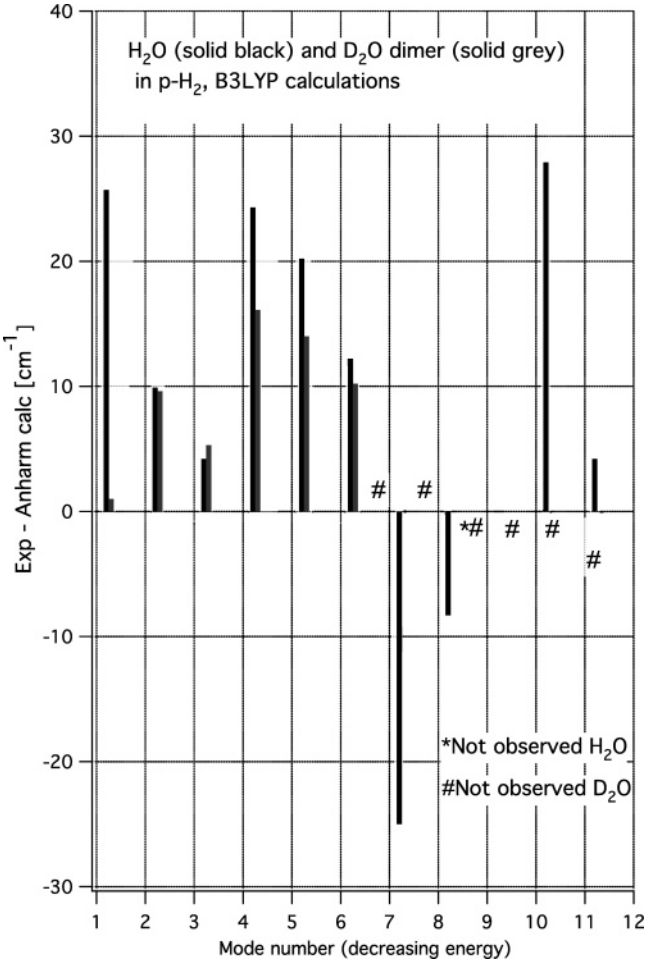

Figure 4. Comparison between experimental normal-mode frequencies of H_2O and D_2O dimers in parahydrogen and calculated normal-mode frequencies. The numbers correspond to the modes shown in Tables 2 and 3.

for the parahydrogen experiments. For D_2O-DOD, the water monomer rotation line is outside the integration interval and no correction is needed.

Mode 3, $\nu_1(H_2O-HOH)$, has a low band strength. It is therefore more sensitive to the choice of baseline and it is also more sensitive to external perturbations. However, it is well separated from monomer bands and therefore the baseline is easy to draw. We believe that the fact that the intensity estimates of both H_2O-HOH and D_2O-DOD are higher in neon than in parahydrogen is real and due to differences in matrix dimer interactions.

Mode 4, $\nu_1(HOH-OH_2)$, is a very strong band which is measurable only at very low dimer concentrations. It is well separated from other bands and there are no particular baseline problems.

The band of mode 5, $\nu_2(HOH-OH_2)$, in neon matrices overlaps the main monomer water band and it is difficult to obtain a correct baseline. This is probably the reason for the low band strength estimate.

Mode 6, $\nu_2(H_2O-HOH)$, is well separated from other bands and has been used to estimate dimer concentrations.

For monomeric water, the calculated band strengths of the bends are 13% higher than the experimental values for both H_2O and for D_2O. The intensities of the symmetric stretches are approximately twice the experimental values, and for the asymmetric stretches the calculated values are 1.25 times the experimental values for both H_2O and D_2O.

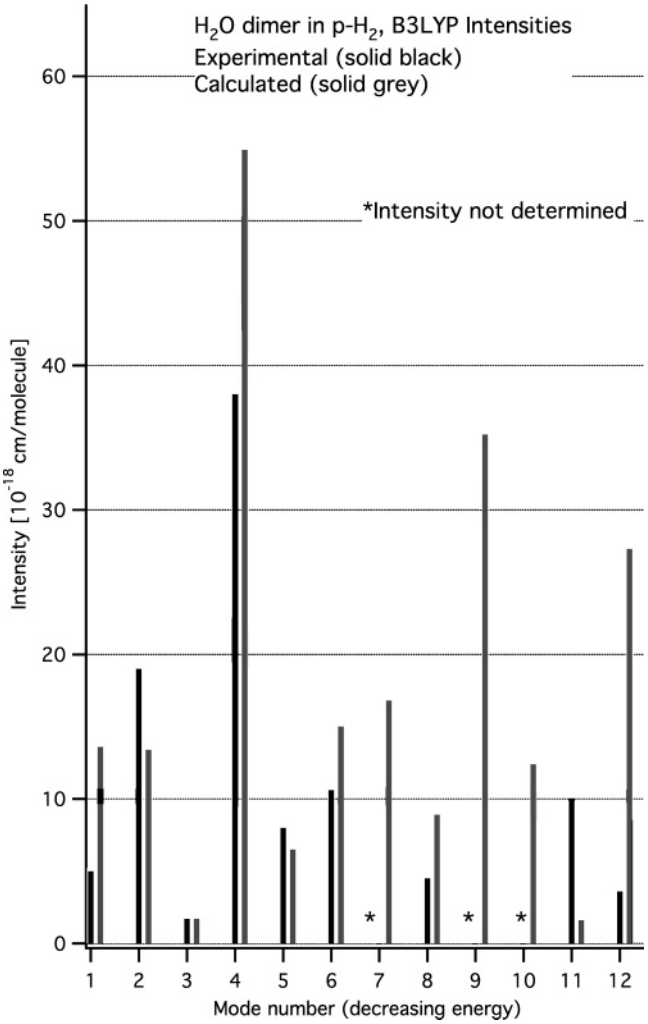

Figure 5. Comparison between experimental normal-mode intensities of H_2O dimer and calculated values. The numbers correspond to the normal modes shown in Table 2.

In Figure 4 the difference of the mode frequencies between the experimental values and the calculated anharmonic values of $(H_2O)_2$ and $(D_2O)_2$ in parahydrogen are presented. For H_2O the agreement is always better than 30 cm^{-1}, and for D_2O it is better than 16 cm^{-1} which is attributed to the reduced anharmonicity of D_2O.

The band strengths obtained from measurements of $(H_2O)_2$ in parahydrogen are compared with the results from our DFT calculations in Figure 5. No correction for the dielectric effect on the measured intensities has been applied since the refractive indices of solid neon and solid hydrogen are close to one.[30] There is a very good qualitative agreement between the experiments and our DFT calculations. All trends are reproduced with the exception of mode 1 and two modes lowest in frequency, that is, 11 and 12. The theoretical description of these two modes is likely to be incorrect. Mode 1, $\nu_3(H_2O-HOH)$, and $\nu_3(D_2O-DOD)$ is temperature dependent and overlapped by water monomer absorption. The estimated band strengths are therefore very uncertain.

The calculated band strengths of $\nu_1(HOH-OH_2)$ are 1.7 times the neon values and 1.4 times the parahydrogen values. For $\nu_2(H_2O-HOH)$ and $\nu_3(HOH-OH_2)$, the calculated values are in reasonable agreement with the experimental values. For $\nu_3(H_2O-HOH)$ the calculations give values far higher than the measurements, and particularly so for D_2O-DOD. Here the measurements may not include the whole band as the monomer absorption may interfere. The bend of the donor, $\nu_2(HOH-OH_2)$, is severely disturbed by monomer absorption for H_2O-HOH in neon; in the remaining cases the agreement between calculations and experiment is reasonable. In the calculations, the band strengths of $\nu_2(H_2O-HOH)$ and $\nu_2(D_2O-DOD)$ increased 1.2 times from the monomer values both for H_2O and D_2O. A corresponding change in band strength between monomer and dimer in the matrix would increase the experimental band strengths with a factor 1.2. For most bands these changes are smaller than the experimental uncertainties. Perhaps the only band which is affected by these considerations is $\nu_1(HOH-OH_2)$ where the agreement between calculations and experiment would improve significantly.

The two upper intermolecular fundamentals of the water dimer are well described by the ab initio calculations. Both positions and intensities are in reasonable agreement with experiment. These motions seem to occur in all binary complexes where water acts as a proton donor [24] and may be described as librations of the proton-donating water molecule around its free OH-bond (out-of-plane-bending) and around an axis orthogonal to the HOH plane through its center of mass, respectively (in-plane-bending). They appear to be well separated from the remaining intermolecular motions. The remaining calculated fundamentals are strongly anharmonic and coupled which make them difficult to determine using first-principal calculations.

In conclusion, we have for the first time measured the normal-mode intensities of all intramolecular modes and most intermolecular modes of the water dimer for both H_2O and D_2O. The intensities are in qualitative agreement with our DFT calculations.

Acknowledgment. This work was supported by Vetenskapsrådet and Crafoordstiftelsen.

References and Notes

(1) Van Thiel, M.; Becker, E. D.; Pimentel, G. C. *J. Chem. Phys.* **1957**, *27*, 486.
(2) Tursi, A. J.; Nixon, E. R. *J. Chem. Phys.* **1970**, *52*, 1521.
(3) Ayers, G. P.; Pullin, A. D. E. *Spectrochim. Acta A* **1976**, *32*, 1629.
(4) Fredin, L.; Nelander, B.; Ribbegård, G. *J. Chem. Phys.* **1977**, *66*, 4065.
(5) Dyke, T. R.; Mack, K. M.; Muenter, J. S. *J. Chem. Phys.* **1977**, *66*, 498.
(6) Morokuma, K.; Pederson, L. *J. Chem. Phys.* **1968**, *48*, 3275.
(7) Smith, B. J.; Swanton, D. J.; Pople, J., A.; Schaeffer, H. F., III; Radom, L. *J. Chem. Phys.* **1990**, *92*, 1240.
(8) Huang, Z. S.; Miller, R. E. *J. Chem. Phys.* **1989**, *91*, 6613.
(9) Huisken, F.; Kaloudis, M.; Kulcke, A. *J. Chem. Phys.* **1996**, *104*, 17.
(10) Paul, J. B.; Provencal, R. A.; Chapo, C.; Roth, K.; Casaes, R.; Saykally, R. J. *J. Phys. Chem. A* **1999**, *103*, 2972.
(11) Braly, L. B.; Liu, K.; Brown, M. G.; Keutsch, F. N.; Fellers, R. S.; Saykally, R. J. *J. Chem. Phys.* **2000**, *112*, 10314 and references therein.
(12) Braly, L. B.; Cruzan, J. D.; Liu, K.; Fellers, R. S.; Saykally, R. J. *J. Chem. Phys.* **2000**, *112*, 10293.
(13) Keutsch, F. N.; Braly, L. B.; Brown, M. G.; Harker, H. A.; Petersen, P. B.; Leforestier, C.; Saykally, R. J. *J. Chem. Phys.* **2003**, *119*, 8927.
(14) Smit, M. J.; Groenenboom, G. C.; Wormer, P. E. S.; van der Avoird, A.; Bukowski, R.; Szalewicz, K. *J. Phys. Chem.* A **2001**, *105*, 6212.
(15) Bentwood, R. M.; Barnes, A. J.; Orville-Thomas, W. J. *J. Mol. Spectrosc.* **1980**, *84*, 391.
(16) Ceponkus, J.; Nelander, B. *J. Phys. Chem.* A **2004**, *108*, 6499.
(17) Bouteiller, Y.; Perchard, J. P. *Chem. Phys.* **2004**, *305*, 1.
(18) Pfeilsticker, K.; Lotter, A.; Peters, C.; Bösch, H. *Science* **2003**, *300*, 2078.
(19) Kjaergaard, H., G.; Robinson, T. W.; Howard, D. L., Daryl L.; Daniel, J. S.; Headrick, J. E.; Vaida, V. *J. Phys. Chem. A* **2003**, *107*, 10680−10686.
(20) Goldman, N.; Leforestier, C.; Saykally, R. J. *J. Phys. Chem. A* **2004**, *108*, 787−794.
(21) Zilles, B. A.; Person, W. B. *J. Chem. Phys.* **1983**, *79*, 65.

(22) Tam, S.; Fajardo, M. E. *Appl. Spectrosc.* **2001**, *55*, 1634.
(23) Wilemski, G. *J. Quant. Spectrosc. Radiat. Transfer* **1978**, *20*, 291.
(24) Åstrand, P.-O.; Karlström, G.; Engdahl, A.; Nelander, B. *J. Chem. Phys.* **1995**, *102*, 3534.
(25) Frisch, M. J.; Trucks, G. W.; Schlegel, H. B.; Scuseria, G. E.; Robb, M. A.; Cheeseman, J. R.; Montgomery, J. J. A.; Vreven, T.; Kudin, K. N.; Burant, J. C.; Millam, J. M.; Iyengar, S. S.; Tomasi, J.; Barone, V.; Mennucci, B.; Cossi, M.; Scalmani, G.; Rega, N.; Petersson, G. A.; Nakatsuji, H.; Hada, M.; Ehara, M.; Toyota, K.; Fukuda, R.; Hasegawa, J.; Ishida, M.; Nakajima, T.; Honda, Y.; Kitao, O.; Nakai, H.; Klene, M.; Li, X.; Knox, J. E.; Hratchian, H. P.; Cross, J. B.; Adamo, C.; Jaramillo, J.; Gomperts, R.; Stratmann, R. E.; Yazyev, O.; Austin, A. J.; Cammi, R.; Pomelli, C.; Ochterski, J. W.; Ayala, P. Y.; Morokuma, K.; Voth, G. A.; Salvador, P.; Dannenberg, J. J.; Zakrzewski, V. G.; Dapprich, S.; Daniels, A. D.; Strain, M. C.; Farkas, O.; Malick, D. K.; Rabuck, A. D.; Raghavachari, K.; Foresman, J. B.; Ortiz, J. V.; Cui, Q.; Baboul, A. G.; Clifford, S.; Cioslowski, J.; Stefanov, B. B.; Liu, G.; Liashenko, A.; Piskorz, P.; Komaromi, I.; Martin, R. L.; Fox, D. J.; Keith, T.; Al-Laham, M. A.; Peng, C. Y.; Nanayakkara, A.; Challacombe, M.; Gill, P. M. W.; Johnson, B.; Chen, W.; Wong, M. W.; Gonzalez, C.; Pople, J. A. *Gaussian 03*; Pittsburg, PA, 2003.
(26) Xu, X.; Goddard, W. A. *J. Phys. Chem. A* **2004**, *108* (12), 2305.
(27) Klopper, W.; van Duijneveldt-van de Rijdt, J. G. C. M.; van Duijneveldt, F. *Phys. Chem. Chem. Phys*. **2000**, *2*, 2227.
(28) Goldman, N.; Fellers, R. S.; Brown, M. G.; Braly, L. B.; Keoshian, C. J.; Leforestier, C.; Saykally, R. J. *J. Chem. Phys.* **2002**, *116*, 10148.
(29) Knözinger, E.; Hoffmann, P.; Huth, M.; Kollhoff. H.; Langel, W.; Schrems, O.; Schuller, W. *Microchim. Acta* **1987**, *III*, 123
(30) Dewaele, A.; Eggert, J. H.; Loubeyre, P.; Le Toullec, R. *Phys. Rev B* **2003**, *67*, 094112.
(31) Benedict, W. S.; Gailar, N.; Plyler, E. K. *J. Chem. Phys*. **1956**, *24*, 1139.